PHYSICAL REVIEW A VOLUME 51, NUMBER 2 FEBRUARY 1995

Relativistic many-body calculations of $[2p^5 3s]$ excited-state energy levels for neonlike ions

E. Avgoustoglou, W.R. Johnson, Z.W. Liu, and J. Sapirstein
Department of Physics, University of Notre Dame, Notre Dame, Indiana 46556

(Received 6 October 1994)

Relativistic many-body perturbation theory is applied to determine energies of $[2p^5 3s]$ excited states of neonlike ions with nuclear charges in the range Z =10–92. These calculations start with a $V^{(N-1)}$ Hartree-Fock potential and include correlation corrections. Core-hole corrections are treated to all orders in perturbation theory while the core-core, valence-core, and valence-hole corrections are treated to second order only. The Breit interaction is also included to second order, but the dominant correlation corrections to the Breit interaction are identified and iterated to all orders. Frequency-dependent corrections to the Breit interaction and mass-polarization corrections are treated to first order only. Lowest-order radiative corrections are included by evaluating the electron self-energy and vacuum polarization in a local potential that approximates the Hartree-Fock potential. Detailed comparisons are made with measurements and with other calculations.

PACS number(s): 31.30.Jv, 12.20.Ds, 31.25.Jf

I. INTRODUCTION

Over the years, there has been considerable experimental [1–41] and theoretical [42–51] interest in the energy levels of excited states of neon and neonlike ions. Recent interest arises in part from the need for precise energy levels in plasma research and in part because the energy levels of neonlike ions provide important tests of relativistic and quantum electrodynamic (QED) corrections in multielectron systems. For the neutral neon atom, the classical work by Paschen [52] in 1920 forms the basis for all subsequent investigations; predictions of neon energy levels have presented challenging tests for atomic-structure calculations ever since. Neonlike ions with $Z < 50$ are important in plasma research due to their stable closed-shell configurations; the corresponding emission lines are essential for diagnostics over a wide range of plasma parameters, from those for Tokamaks to those for solar flares [2–35]. For neonlike ions with $Z > 50$, a series of high-resolution measurements has been made recently [36–41]. Because the Coulomb and Breit contributions to the correlation energy for high-Z ions can be treated accurately, a systematic comparison of experimental and theoretical transition energies offers a method to test our understanding of QED corrections in highly charged many-electron ions.

Excited states of closed-shell atoms or ions, such as those of the neon sequence, can be conveniently treated using a particle-hole formalism [51,53] within the framework of many-body perturbation theory (MBPT). An electron is removed from one of the closed shells, creating a hole. This electron is excited into a valence orbital, leading to a particle-hole excited state of the closed-shell atom. In a perturbation expansion, starting from the independent-particle approximation, one divides the correlation corrections for particle-hole states into four sectors: core-core, core-hole, valence-core, and valence-hole. Higher-order correction terms in each of these sectors may be evaluated either by using an order-by-order expansion or by using all-order methods [54]. The valence-core and valence-hole sectors must be treated by open-shell MBPT, which is usually complex [55]. In particular, inclusion of the valence-core and valence-hole sectors leads to the so-called *redundancy* problem [53], the nonuniqueness of the valence correlation amplitudes.

In this paper, we notice that if a proper choice of the starting potential is made the calculation can be considerably simplified. Thus, if we start with a $V^{(N-1)}$ Hartree-Fock (HF) potential, in which all virtual orbitals are generated in the field of the hole state [56], the dominant contribution to the correlation correction comes from the core-hole sector alone. When correlation corrections from the core-core, valence-core, and valence-hole sectors are taken into account to second order and correlation corrections from the core-hole sector are evaluated to all orders, accurate results for excited-state energies for neutral neon and neonlike ions are obtained. In this way, the entire calculation is reduced to a problem that is almost as simple as that for a closed-shell atom.

After determining the electrostatic contributions to the excited-state energies by solving the all-order equations, we evaluate the Breit contributions and the second-order Breit-Coulomb correlation corrections. We find that the second-order Breit-Coulomb correction is dominated by a single term. This term is iterated to give the dominant third- and higher-order Breit-Coulomb correlation corrections. Next, the frequency-dependent corrections to the Breit interaction and the lowest-order radiative corrections are considered. These QED corrections are evaluated in a local potential that approximates the $V^{(N-1)}$ HF potential. Finally, reduced-mass and mass-polarization corrections are determined in lowest order.

The resulting theoretical energies are in excellent agreement with measurement for $Z < 50$. We find that the theoretical energy levels are systematically smaller than the measured ones for each of the four states considered. The energy differences grow from ≈ 0.001 a.u. near the neutral end of the sequence to ≈ 0.01 a.u. near $Z = 50$ and increase to ≈ 0.1 a.u. at $Z = 90$. Although we have no explanation for the relatively large differences near $Z = 90$, we note that 0.1 a.u. differences between MBPT calculations and experiment have been reported recently for other transitions in neonlike uranium [57].

The plan of this paper is as follows: In Sec. II, we present the detailed MBPT formulas and describe our treatment of the Breit interaction, mass polarization, and QED corrections. Then, in Sec. III, we present the results of our calculations and make comparisons with experiment and with other recent calculations.

II. FORMALISM

We start our calculations using a set of unperturbed state vectors and energies obtained from the independent-particle approximation [54]. In this approximation, each electron interacts individually with a spherically symmetric model potential $U(r)$ that accounts approximately for the interaction with the other electrons of the system. Here, we choose the model potential to be the $V^{(N-1)}$ Hartree-Fock potential of the closed-shell atom.

Relativistically, an N-electron atom is described by the "no-pair" Hamiltonian [58], which may be written

$$H = H_0 + V_I, \tag{2.1}$$

where, in second-quantized form,

$$H_0 = \sum_i \varepsilon_i a_i^\dagger a_i, \tag{2.2}$$

and

$$V_I = \frac{1}{2}\sum_{ijkl} g_{ijkl} a_i^\dagger a_j^\dagger a_l a_k - \sum_{ij} U_{ij} a_i^\dagger a_j. \tag{2.3}$$

In Eq. (2.2), ε_i is the eigenvalue of the one-electron Dirac equation

$$h(\mathbf{r})\,\varphi_i(\mathbf{r}) = \varepsilon_i\,\varphi_i(\mathbf{r}), \tag{2.4}$$

where the Dirac Hamiltonian $h(\mathbf{r})$ includes not only the interaction with the nucleus $V_{\rm nuc}(r)$, but also the interaction with the model potential $U(r)$,

$$h(\mathbf{r}) = c\boldsymbol{\alpha}\cdot\boldsymbol{p} + (\beta - 1)c^2 + V_{\rm nuc}(r) + U(r). \tag{2.5}$$

The quantities $\boldsymbol{\alpha}$ and β are 4×4 Dirac matrices in standard representation. The nuclear potential $V_{\rm nuc}(r)$ is taken to be that of a finite Fermi charge distribution with 90–10 % falloff thickness $t = 2.3$ fm and with root-mean-square radius taken from Ref. [59].

In Eq. (2.3), the quantity U_{ij} is a one-electron matrix element of the model potential $U(r)$,

$$U_{ij} = \int \varphi_i^\dagger(\mathbf{r})U(r)\varphi_j(\mathbf{r})d^3r, \tag{2.6}$$

and g_{ijkl} is a two-electron matrix element of the Coulomb interaction,

$$g_{ijkl} = \int\!\!\int \frac{d^3r_1 d^3r_2}{r_{12}}\varphi_i^\dagger(\mathbf{r}_1)\varphi_j^\dagger(\mathbf{r}_2)\varphi_k(\mathbf{r}_1)\varphi_l(\mathbf{r}_2). \tag{2.7}$$

In Eqs. (2.2) and (2.3), the quantities $a_i^\dagger$ and a_i denote electron creation and annihilation operators, respectively. The corresponding positron creation and annihilation operators are excluded from the no-pair Hamiltonian. The index i that accompanies these operators represents the collection (n_i, κ_i, m_i), which are the principal, angular, and magnetic quantum numbers, respectively, of the corresponding orbital. To distinguish between different categories of orbitals, we use the following index conventions: indices a and v represent the hole and valence states, respectively; $r, s, t, \ldots$ represent virtual states; $b, c, d, \ldots$ represent core states; $\alpha, \beta, \gamma, \ldots$ represent either hole or virtual states; and $i, j, k, \cdots$ represent all orbitals. We also introduce the notation that a four-index quantity with a tilde represents an antisymmetrized form of the quantity. Thus, for example, $\tilde{g}_{ijkl} = g_{ijkl} - g_{ijlk}$.

A. Coulomb interaction

To obtain the Coulomb correlation corrections, we must solve the time-independent Schrödinger equation:

$$H|\Psi(JM)\rangle = E|\Psi(JM)\rangle. \tag{2.8}$$

For the particle-hole case, we take our lowest-order model space state vectors [60] to be

$$|\Phi_{av}(JM)\rangle = F_{av} a_v^\dagger a_a |0_c\rangle, \tag{2.9}$$

where the operator F_{av} is given by

$$F_{av} = \sum_{m_a m_v} (-1)^{j_a - m_a}\langle j_v m_v, j_a - m_a|JM\rangle, \tag{2.10}$$

and where $|0_c\rangle$ denotes the closed-shell state vector for the ground state of the neonlike ion.

In previous work [51], we assumed that there was no mixing of states in lowest-order, so that a and v could be considered unique. In many cases of interest, however, there is significant mixing between states with different quantum numbers. For example, in low-Z neonlike ions, the states $[2p_{3/2}^{-1}3s_{1/2}]_{J=1}$ and $[2p_{1/2}^{-1}3s_{1/2}]_{J=1}$ are nearly degenerate. In such cases, the solution to the Schrödinger equation is obtained by letting the wave operator Ω_{av} act on a linear combination of the nearly degenerate model states [61]. The particle-hole state vector becomes

$$|\Psi(JM)\rangle = \sum_{av} C_{av}\Omega_{av}|\Phi_{av}(JM)\rangle. \tag{2.11}$$

Equation (2.11) can be rewritten with the help of the correlation operator χ_{av} defined through

$$\Omega_{av} = 1 + \chi_{av}. \tag{2.12}$$

From Schrödinger's equation (2.8), with the aid of relations (2.11) and (2.12), we obtain an equation for the correlation operator:

$$[\chi_{av}, H_0]|\Phi_{av}(JM)\rangle = V_I(1+\chi_{av})|\Phi_{av}(JM)\rangle - \sum_{a',v'} \chi_{a'v'}|\Phi_{a'v'}(JM)\rangle\langle\Phi_{a'v'}(JM)|V(1+\chi_{av})|\Phi_{av}(JM)\rangle, \qquad (2.13)$$

and the eigenvalue equation

$$\sum_{av} H^{\text{eff}}_{a'v',av} C_{av} = E C_{a'v'}, \qquad (2.14)$$

where the effective Hamiltonian H^{eff} is given by

$$H^{\text{eff}}_{a'v',av} = \langle\Phi_{a'v'}(JM)|H(1+\chi_{av})|\Phi_{av}(JM)\rangle. \qquad (2.15)$$

Here, we approximate the correlation operator by considering single and double excitations only:

$$\chi \approx \sum_{ij} a_i^\dagger a_j \chi_j^i + \frac{1}{2}\sum_{ijkl} a_i^\dagger a_j^\dagger a_l a_k \chi_{kl}^{ij}. \qquad (2.16)$$

Applying this operator to the lowest-order state vector (2.9), we obtain

$$\begin{aligned}\chi_{av}|\Phi_{av}(JM)\rangle = {} & \sum_{rb} \chi_b^r a_r^\dagger a_b a_v^\dagger a_a|0_c\rangle + \sum_{b\neq a} \chi_b^a a_b a_v^\dagger|0_c\rangle + \sum_{r\neq v} \chi_v^r a_r^\dagger a_a|0_c\rangle + \chi_v^a|0_c\rangle \\ & + \sum_{rsb} \chi_{vb}^{rs} a_r^\dagger a_s^\dagger a_b a_a|0_c\rangle + \sum_{sb\neq va} \tilde{\chi}_{vb}^{as} a_s^\dagger a_b|0_c\rangle \\ & + \frac{1}{2}\sum_{rsbc} \chi_{bc}^{rs} a_r^\dagger a_s^\dagger a_c a_b a_v^\dagger a_a|0_c\rangle + \sum_{sbc} \chi_{bc}^{as} a_s^\dagger a_c a_b a_v^\dagger|0_c\rangle. \end{aligned} \qquad (2.17)$$

Equation (2.17) unveils an issue for open-shell systems [53] referred to as the *redundancy problem* that has to do with an ambiguity between different sectors of the correlation operator. On comparing the third and sixth terms of Eq. (2.17), it is seen that the coefficients χ_v^r and $\tilde{\chi}_{vb}^{as}$ refer to the same state when $b = a$. The resulting ambiguity is resolved by imposing the additional constraint $b \neq a$ on the pair coefficient $\tilde{\chi}_{vb}^{as}$ and adding the excluded terms to the corresponding single-excitation coefficients. Thus, χ_v^r is replaced by $\chi_v^r + \tilde{\chi}_{va}^{ar}$.

Relations (2.13) and (2.17) lead to a system of coupled equations for the correlation coefficients:

$$(\varepsilon_b - \varepsilon_\alpha)\chi_b^\alpha = \mathcal{R}_b^\alpha, \qquad (2.18)$$

$$(\varepsilon_b + \varepsilon_c - \varepsilon_\alpha - \varepsilon_\beta)\chi_{bc}^{\alpha\beta} = \mathcal{R}_{bc}^{\alpha\beta}, \qquad (2.19)$$

$$(\varepsilon_v - \varepsilon_r)\chi_v^r = \mathcal{R}_v^r - \sum_{v'a'} \delta_{aa'}\chi_{v'}^r \mathcal{W}_{va'}^{v'a}, \qquad (2.20)$$

$$(\varepsilon_v + \varepsilon_b - \varepsilon_r - \varepsilon_s)\chi_{vb}^{rs} = \mathcal{R}_{vb}^{rs} - \sum_{v'a'} \delta_{aa'}\chi_{v'b}^{rs} \mathcal{W}_{va'}^{v'a}, \qquad (2.21)$$

$$(\varepsilon_a - \varepsilon_v)\chi_v^a = \mathcal{R}_v^a - \sum_{v'a'} \chi_{v'}^{a'} \mathcal{W}_{va'}^{v'a}, \qquad (2.22)$$

$$(\varepsilon_v + \varepsilon_b - \varepsilon_a - \varepsilon_s)\chi_{vb}^{as} = \mathcal{R}_{vb}^{as} - \sum_{v'a'} \chi_{v'b}^{a's} \mathcal{W}_{va'}^{v'a}, \qquad (2.23)$$

where

$$\mathcal{W}_{va'}^{v'a} = \mathcal{R}_v^{v'}\delta_{a'a} - \mathcal{R}_{a'}^a\delta_{v'v} + \tilde{\mathcal{R}}_{va'}^{av'}. \qquad (2.24)$$

The effective Hamiltonian can be written

$$H^{\text{eff}}_{v'a',va} = (\varepsilon_v - \varepsilon_a)\delta_{v'v}\delta_{a'a} + \mathcal{W}_{va'}^{v'a}. \qquad (2.25)$$

The single-excitation correlation term is defined as

$$\begin{aligned}\mathcal{R}_j^i = {} & \Delta_{ij} + \sum_s \Delta_{is}\chi_j^s - \sum_c \Delta_{cj}\chi_c^i + \sum_{sc} \Delta_{cs}\tilde{\chi}_{jc}^{is} \\ & + \sum_{sc} \tilde{g}_{icjs}\chi_c^s - \sum_{scd} g_{cdjs}\tilde{\chi}_{cd}^{is} \\ & + \sum_{stc} g_{icst}\tilde{\chi}_{jc}^{st}, \end{aligned} \qquad (2.26)$$

and the pair-excitation correlation term as

$$\begin{aligned}\mathcal{R}_{kl}^{ij} = {} & g_{ijkl} + \sum_{tu} g_{ijtu}\chi_{kl}^{tu} + \sum_{cd} g_{cdkl}\chi_{cd}^{ij} \\ & + \left[\Delta_{ik}\chi_l^j + \sum_t \Delta_{it}\chi_{kl}^{tj} - \sum_d \Delta_{dk}\chi_{dl}^{ij}\right. \\ & + \sum_t g_{ijtl}\chi_k^t - \sum_d g_{djkl}\chi_d^i \\ & \left. + \sum_{td} \tilde{g}_{djtl}\tilde{\chi}_{kd}^{it} + (i \rightleftharpoons j, k \rightleftharpoons l)\right], \end{aligned} \qquad (2.27)$$

where the notation $\rightleftharpoons$ denotes the terms identical to the previous ones but with the corresponding indices interchanged. In Eqs. (2.26) and (2.27),

$$\Delta_{ij} = \sum_b \tilde{g}_{ibjb} - U_{ij}. \qquad (2.28)$$

When $U(r)$ is chosen to be the $V^{(N-1)}$ HF potential, we find that

$$\Delta_{ij} = \begin{cases} \tilde{g}_{ihjh} & \text{if } i,j \notin \text{core}, \\ 0 & \text{otherwise} . \end{cases} \tag{2.29}$$

Here, h is index of the the hole state used to generate the $V^{(N-1)}$ HF potential. In our calculations, we construct this potential with a hole in the $2p_{3/2}$ state.

To compute the correlation coefficients, we iterate Eqs. (2.18)–(2.23). Once convergence is obtained, these coefficients are used in the effective Hamiltonian matrix (2.25). On diagonalizing this matrix, we obtain the transition energies and the mixing coefficients between the states under consideration.

In lowest order, we write $\mathcal{R}^i_j \approx \Delta_{ij}$ and $\mathcal{R}^{ij}_{kl} \approx g_{ijkl}$. Using these values, we obtain as an approximation for the effective Hamiltonian,

$$\begin{aligned} H^{\text{eff}}_{v'a',va} \approx (\varepsilon_v - \varepsilon_a)\delta_{v'v}\delta_{a'a} + \Delta_{v'v}\delta_{a'a} \\ -\Delta_{aa'}\delta_{v'v} + \tilde{g}_{v'aa'v} . \end{aligned} \tag{2.30}$$

The eigenvalues of this matrix give us the first approximation to the energy. In Table I, we list the corresponding eigenvalues as $E^{(0)} + E^{(1)}$.

If we use the lowest-order approximation above for $\mathcal{R}^i_j$ and $\mathcal{R}^{ij}_{kl}$ to obtain a first approximation for the correlation operators, we find

$$\begin{aligned} \chi^{ij}_{kl} &\approx \frac{g_{ijkl}}{\varepsilon_k + \varepsilon_l - \varepsilon_i - \varepsilon_j} , \\ \chi^i_j &\approx \frac{\Delta_{ij}}{\varepsilon_j - \varepsilon_i} . \end{aligned}$$

Using these expressions, we obtain second approximations for $\mathcal{R}^i_j$ and $\mathcal{R}^{ij}_{kl}$:

$$\begin{aligned} \mathcal{R}^i_j \approx \Delta_{ij} &+ \sum_s \frac{\Delta_{is}\Delta_{sj}}{\varepsilon_j - \varepsilon_s} - \sum_c \frac{\Delta_{cj}\Delta_{ic}}{\varepsilon_c - \varepsilon_i} + \sum_{cs} \frac{\Delta_{cs}\tilde{g}_{isjc}}{\varepsilon_j + \varepsilon_c - \varepsilon_i - \varepsilon_s} + \sum_{cs} \frac{\tilde{g}_{icjs}\Delta_{sc}}{\varepsilon_c - \varepsilon_s} \\ &- \sum_{scd} \frac{g_{cdjs}\tilde{g}_{iscd}}{\varepsilon_c + \varepsilon_d - \varepsilon_i - \varepsilon_s} + \sum_{stc} \frac{g_{icst}\tilde{g}_{stjc}}{\varepsilon_j + \varepsilon_c - \varepsilon_s - \varepsilon_t} , \end{aligned} \tag{2.31}$$

and

$$\begin{aligned} \mathcal{R}^{ij}_{kl} \approx g_{ijkl} &+ \sum_{tu} \frac{g_{ijtu}g_{tukl}}{\varepsilon_k + \varepsilon_l - \varepsilon_t - \varepsilon_u} + \sum_{cd} \frac{g_{cdkl}g_{ijcd}}{\varepsilon_c + \varepsilon_d - \varepsilon_i - \varepsilon_j} \\ &+ \left[\frac{\Delta_{ik}\Delta_{jl}}{\varepsilon_l - \varepsilon_j} + \sum_t \frac{\Delta_{it}g_{tjkl}}{\varepsilon_k + \varepsilon_l - \varepsilon_t - \varepsilon_j} - \sum_d \frac{\Delta_{dk}g_{ijdl}}{\varepsilon_d + \varepsilon_l - \varepsilon_i - \varepsilon_j} \right. \\ &\left. + \sum_t \frac{g_{ijtl}\Delta_{tk}}{\varepsilon_k - \varepsilon_t} - \sum_d \frac{g_{djkl}\Delta_{id}}{\varepsilon_d - \varepsilon_i} + \sum_{td} \frac{\tilde{g}_{djtl}\tilde{g}_{itkd}}{\varepsilon_k + \varepsilon_d - \varepsilon_i - \varepsilon_t} + (i \rightleftharpoons j, k \rightleftharpoons l) \right] . \end{aligned} \tag{2.32}$$

For the special case of the $V^{(N-1)}$ HF potential, these expressions lead to

$$\mathcal{R}^{v'}_v \approx \Delta_{v'v} + \sum_s \frac{\Delta_{v's}\Delta_{sv}}{\varepsilon_v - \varepsilon_s} - \sum_{scd} \frac{g_{cdvs}\tilde{g}_{v'scd}}{\varepsilon_c + \varepsilon_d - \varepsilon'_v - \varepsilon_s} + \sum_{stc} \frac{g_{v'cst}\tilde{g}_{stvc}}{\varepsilon_v + \varepsilon_c - \varepsilon_s - \varepsilon_t} , \tag{2.33}$$

$$\mathcal{R}^a_{a'} \approx - \sum_{scd} \frac{g_{cda's}\tilde{g}_{ascd}}{\varepsilon_c + \varepsilon_d - \varepsilon_a - \varepsilon_s} + \sum_{stc} \frac{g_{acst}\tilde{g}_{sta'c}}{\varepsilon'_a + \varepsilon_c - \varepsilon_s - \varepsilon_t} , \tag{2.34}$$

$$\begin{aligned} \tilde{\mathcal{R}}^{av'}_{va'} \approx \tilde{g}_{av'va'} &+ \sum_{tu} \frac{g_{av'tu}\tilde{g}_{tuva'}}{\varepsilon_v + \varepsilon'_a - \varepsilon_t - \varepsilon_u} + \sum_{cd} \frac{\tilde{g}_{cdva'}g_{av'cd}}{\varepsilon_c + \varepsilon_d - \varepsilon_a - \varepsilon'_v} \\ &+ \sum_t \frac{\tilde{g}_{av'ta'}\Delta_{tv}}{\varepsilon_v - \varepsilon_t} + \sum_{td} \frac{\tilde{g}_{dv'ta'}\tilde{g}_{atvd}}{\varepsilon_v + \varepsilon_d - \varepsilon_a - \varepsilon_t} - \sum_{td} \frac{\tilde{g}_{dv'tv}\tilde{g}_{ata'd}}{\varepsilon'_a + \varepsilon_d - \varepsilon_a - \varepsilon_t} \\ &+ \sum_t \frac{\Delta_{v't}\tilde{g}_{taa'v}}{\varepsilon_v + \varepsilon'_a - \varepsilon_t - \varepsilon_a} + \sum_{td} \frac{\tilde{g}_{datv}\tilde{g}_{v'ta'd}}{\varepsilon'_a + \varepsilon_d - \varepsilon'_v - \varepsilon_t} - \sum_{td} \frac{\tilde{g}_{data'}\tilde{g}_{v'tvd}}{\varepsilon_v + \varepsilon_d - \varepsilon'_v - \varepsilon_t} . \end{aligned} \tag{2.35}$$

Substituting Eqs. (2.33) and (2.34) into Eq. (2.24) leads to a second-order approximation for the effective Hamiltonian. In our numerical calculations, the multiple sums over excited states u and t are carried out with the aid of finite basis methods. [62] The eigenvalues of the second-order effective Hamiltonian are written $E^{(0)} + E^{(1)} + E^{(2)}$. The resulting values of $E^{(2)}$ for the states considered are listed in Table I. Formulas for the second-order energies obtained from the iterative scheme outlined here agree precisely with results of conventional second-order MBPT [51]. The next iteration of the coupled equations, however, leads to results that differ from conventional third-order perturbation theory. The differences are accounted for by the fact that we include only single and double excitations here, whereas contributions from triple excitations also occur in third-order perturbation theory.

For highly charged ions, second-order MBPT energies are found to be very close to the iterative results. This is not the case in neutral and low-Z systems. Therefore, for low-Z cases, we must carry the iteration further to obtain accurate energies. For all Z, we found that the dominant contribution to the second-order energy arises from the core-hole contribution to the interaction energy given in Eq. (2.34). Therefore, we can obtain the dominant correlation corrections by iterating only that subset of the equations corresponding to core-hole interactions and using the lowest-order values for the remaining correlation coefficients. Specifically, we iterate Eq. (2.18) and those terms in Eq. (2.19) corresponding to $\alpha = a$ or $\beta = a$, and replace all other correlation coefficients by their lowest-order values. In this way, we obtain accurate energies using only modest computer resources. The higher-order energies, designated by $E^{(3+)}$ in Table I, are all calculated in this approximation.

The largest contribution in the right-hand side of Eq. (2.19) is the term that describes the interaction between the hole and other *core* states. For neutral systems,

TABLE I. Contributions to transition energies (a.u.) of the $[2p_{3/2}^{-1}3s_{1/2}]_2$, (2); $[2p_{3/2}^{-1}3s_{1/2}]_1$, (1L); $[2p_{1/2}^{-1}3s_{1/2}]_0$, (0); and $[2p_{1/2}^{-1}3s_{1/2}]_1$, (1U) states of neonlike ions from zeroth- through second-order Coulomb energy, $E^{(0+1)}$ and $E^{(2)}$, all-order hole-core Coulomb correlation energy, $E^{(3+)}$, first- and second-order frequency-independent Breit energy, $B^{(1)}$ and $B^{(2)}$, RPA correction to the frequency-independent Breit energy, $B^{(3+)}$, first-order frequency-dependent Breit energy, ΔB_ω, the QED correction term, "QED", and the reduced-mass and mass-polarization correction, "RM." The sum of these terms, "Total," is the theoretical energy of the states relative to the ground state.

Z	State	$E^{(0+1)}$	$E^{(2)}$	$E^{(3+)}$	$B^{(1)}$	$B^{(2)}$	$B^{(3+)}$	ΔB_ω	QED	RM	Total
10	(2)	0.6614	−0.1590	0.1080	−0.0006	0.0013	−0.0006	0.0000	0.0000	0.0001	0.6106
10	(1L)	0.6640	−0.1602	0.1085	−0.0007	0.0013	−0.0006	0.0000	0.0000	0.0001	0.6124
10	(0)	0.6659	−0.1595	0.1078	−0.0009	0.0012	−0.0007	0.0000	0.0000	0.0001	0.6140
10	(1U)	0.6753	−0.1674	0.1100	−0.0007	0.0012	−0.0007	0.0000	0.0000	0.0001	0.6177
20	(2)	12.8222	−0.0673	0.0148	−0.0102	0.0051	−0.0007	0.0001	0.0010	0.0001	12.7650
20	(1L)	12.8661	−0.0716	0.0153	−0.0105	0.0050	−0.0007	0.0001	0.0010	0.0001	12.8048
20	(0)	12.9643	−0.0697	0.0152	−0.0145	0.0049	−0.0008	0.0000	0.0013	0.0001	12.9007
20	(1U)	13.0053	−0.0761	0.0159	−0.0144	0.0049	−0.0008	0.0000	0.0013	0.0001	12.9361
30	(2)	38.7013	−0.0629	0.0079	−0.0428	0.0121	−0.0010	0.0006	0.0047	0.0001	38.6200
30	(1L)	38.7958	−0.0709	0.0084	−0.0422	0.0119	−0.0010	0.0006	0.0047	0.0001	38.7073
30	(0)	39.6160	−0.0690	0.0084	−0.0611	0.0120	−0.0011	0.0001	0.0067	0.0001	39.5120
30	(1U)	39.6722	−0.0750	0.0087	−0.0627	0.0119	−0.0011	0.0001	0.0067	0.0001	39.5609
40	(2)	78.0421	−0.0611	0.0054	−0.1124	0.0222	−0.0014	0.0028	0.0135	0.0001	77.9112
40	(1L)	78.1768	−0.0640	0.0057	−0.1106	0.0221	−0.0014	0.0028	0.0135	0.0001	78.0450
40	(0)	81.3375	−0.0742	0.0060	−0.1631	0.0226	−0.0015	0.0004	0.0200	0.0001	81.1479
40	(1U)	81.4068	−0.0732	0.0062	−0.1681	0.0224	−0.0015	0.0004	0.0200	0.0002	81.2131
50	(2)	130.4621	−0.0586	0.0041	−0.2322	0.0351	−0.0018	0.0091	0.0293	0.0001	130.2473
50	(1L)	130.6423	−0.0621	0.0044	−0.2282	0.0349	−0.0018	0.0091	0.0293	0.0001	130.4281
50	(0)	139.2705	−0.0959	0.0049	−0.3237	0.0372	−0.0020	0.0011	0.0445	0.0002	138.9368
50	(1U)	139.3769	−0.0831	0.0051	−0.3538	0.0369	−0.0020	0.0011	0.0445	0.0002	139.0258
60	(2)	195.3867	−0.0554	0.0033	−0.4149	0.0509	−0.0022	0.0236	0.0526	0.0002	195.0447
60	(1L)	195.6142	−0.0597	0.0035	−0.4072	0.0505	−0.0022	0.0237	0.0526	0.0002	195.2755
60	(0)	215.2916	−0.0880	0.0043	−0.6443	0.0565	−0.0025	0.0024	0.0826	0.0003	214.7029
60	(1U)	215.4275	−0.0829	0.0045	−0.6632	0.0562	−0.0025	0.0024	0.0826	0.0003	214.8249
70	(2)	271.9485	−0.0518	0.0027	−0.6717	0.0692	−0.0026	0.0526	0.0846	0.0002	271.4317
70	(1L)	272.2308	−0.0616	0.0029	−0.6573	0.0675	−0.0026	0.0527	0.0846	0.0002	271.7172
70	(0)	311.8748	−0.0983	0.0040	−1.0970	0.0816	−0.0032	0.0040	0.1345	0.0005	310.9010
70	(1U)	312.0209	−0.0862	0.0041	−1.1343	0.0815	−0.0032	0.0040	0.1345	0.0005	311.0219
80	(2)	358.8185	−0.0478	0.0023	−1.0108	0.0898	−0.0031	0.1047	0.1265	0.0002	358.0802
80	(1L)	359.1536	−0.0566	0.0024	−0.9885	0.0876	−0.0031	0.1048	0.1265	0.0003	358.4271
80	(0)	432.8908	−0.1107	0.0039	−1.7632	0.1145	−0.0040	0.0046	0.1961	0.0007	431.3328
80	(1U)	433.0641	−0.0972	0.0040	−1.8258	0.1141	−0.0040	0.0047	0.1961	0.0007	431.4568
90	(2)	453.9185	−0.0434	0.0019	−1.4350	0.1120	−0.0037	0.1907	0.1810	0.0003	452.9223
90	(1L)	454.3127	−0.0512	0.0020	−1.4027	0.1095	−0.0037	0.1910	0.1810	0.0004	453.3390
90	(0)	584.1959	−0.1262	0.0040	−2.7282	0.1579	−0.0050	0.0004	0.2543	0.0012	581.7544
90	(1U)	584.3993	−0.1102	0.0041	−2.8298	0.1573	−0.0050	0.0007	0.2543	0.0012	581.8719

this strong interaction led to convergence problems in the iteration solution to Eq. (2.19). Therefore, for those coefficients with $\alpha = a$ and b or $c = a$ or $\beta = a$ and b or $c = a$, we replace Eq. (2.19) with the mathematically equivalent expression

$$(\epsilon_b + \epsilon_c - \epsilon_\alpha - \epsilon_\beta - g_{bcbc})\chi_{bc}^{\alpha\beta} = \mathcal{R}_{bc}^{\alpha\beta} - g_{bcbc}\chi_{bc}^{\alpha\beta} \,. \quad (2.36)$$

The iterative solution to this equation converges more rapidly than that of the original equation.

B. Breit interaction

The Breit interaction is introduced into the no-pair Hamiltonian by adding the term

$$V_B = \frac{1}{2}\sum_{ijkl} b_{ijkl} a_i^\dagger a_j^\dagger a_l a_k \,, \quad (2.37)$$

to the Coulomb interaction Hamiltonian V_I. Here b_{ijkl} is a two-particle matrix element of instantaneous Breit operator $b(\mathbf{r}_{12})$,

$$b(\mathbf{r}_{12}) = -\frac{1}{2r_{12}}\left[\alpha_1 \cdot \alpha_2 + \alpha_1 \cdot \hat{r}_{12}\alpha_2 \cdot \hat{r}_{12}\right]. \quad (2.38)$$

The Breit interaction leads to small corrections to the energy levels that are treated only to first order in V_B but to higher order in V_I.

The various corrections to the Breit interaction are obtained by replacing V_I with $V_I + V_B$ in the many-body Hamiltonian, carrying out an order-by-order perturbation expansion for the energy, then linearizing (in V_B) the resulting terms in the energy expansion. In this way, we obtain for the first-order Breit correction

$$\begin{aligned} B^{(1)} = {} & \sum_{av}\Big[(B_{\mathrm{HF}})_{vv} - (B_{\mathrm{HF}})_{aa}\Big]C_{av}^2 \\ & + \sum_{\substack{a'v' \\ av}} \tilde{b}_{v'aa'v} C_{a'v'} C_{av}, \end{aligned} \quad (2.39)$$

where C_{av} are the expansion coefficients from the first-order Coulomb energy and

$$(B_{\mathrm{HF}})_{ij} = \sum_c \tilde{b}_{icjc} = -\sum_c b_{iccj} \,. \quad (2.40)$$

Numerical values of $B^{(1)}$ are listed in Table I. For particle-hole states in neonlike ions, the dominant contribution to $B^{(1)}$ is from the term $(B_{\mathrm{HF}})_{aa}$, which accounts for between 80% and 90% of the entire term.

The second-order Breit correction $B^{(2)}$, also listed in Table I is obtained by linearizing the expression for the second-order Breit + Coulomb energy in the Breit interaction. This correction is also dominated by a single term, which can be identified as the second-order random-phase-approximation (RPA) correction to the core-hole Breit interaction. For a single channel case, this particular contribution is given by

$$(B_{\mathrm{RPA}}^{(2)})_{aa} = -2\sum_{mb}\frac{(B_{\mathrm{HF}})_{mb}\tilde{g}_{amab}}{\varepsilon_b - \varepsilon_m}. \quad (2.41)$$

The second-order RPA correction contributes about 90% of the entire second-order Breit energy. Moreover, the second-order Breit interaction is a substantial fraction of the first-order Breit interaction, ranging from 100% near the neutral end of the spectrum to about 10% for $Z = 92$.

Because of the relatively large size of the second-order RPA correction, we also include third- and higher-order RPA corrections in our calculations. These higher-order contributions are included by solving the Breit RPA equations,

$$(B_{\mathrm{RPA}})_{na} = (B_{\mathrm{HF}})_{na} + \sum_{mb}\frac{(B_{\mathrm{RPA}})_{mb}[\tilde{g}_{nmab} + \tilde{g}_{nbam}]}{\varepsilon_b - \varepsilon_m}. \quad (2.42)$$

Once these equations have been solved, the RPA correction to the core-hole Breit energy is given by

$$\delta E_{\mathrm{RPA}} = -2\sum_{mb}\frac{(B_{\mathrm{RPA}})_{mb}\tilde{g}_{amab}}{\varepsilon_b - \varepsilon_m}. \quad (2.43)$$

If we ignore the Coulomb interaction, $(B_{\mathrm{RPA}})_{na} \to (B_{\mathrm{HF}})_{na}$. In this approximation, $\delta E_{\mathrm{RPA}} = (B_{\mathrm{RPA}}^{(2)})_{aa}$. The difference $\delta E_{\mathrm{RPA}} - (B_{\mathrm{RPA}}^{(2)})_{aa}$ gives the third- and higher-order RPA corrections to the Breit interaction. We designate this difference as $B^{(3+)}$ in Table I.

C. QED corrections

The QED effects of electron self-energy, vacuum polarization, and frequency dependence of the Breit interaction were evaluated in a local potential that approximates the $V^{(N-1)}$ HF potential. This potential is defined by

$$U(r) = \sum_b (2j_b + 1)v_0(b, r) - v_0(h, r) \,, \quad (2.44)$$

where h designates the $2p_{3/2}$ state and where

$$\begin{aligned} v_0(c, r) = {} & \frac{1}{r}\int_0^r dr'[G_c^2(r') + F_c^2(r')] \\ & + \int_r^\infty \frac{dr'}{r'}[G_c^2(r') + F_c^2(r')]. \end{aligned} \quad (2.45)$$

Here, $G_c(r)$ and $F_c(r)$ are the large and small components of the radial Dirac orbital for state c. The potential $U(r)$ and the core orbitals are calculated self-consistently using standard methods.

1. *Frequency-dependent Breit correction*

Since $U(r)$ is a local potential, the frequency dependence of the Breit interaction can be obtained by calculating one-photon exchange in Feynman gauge and then subtracting the instantaneous Coulomb and Breit interactions. The first-order corrections calculated in this way are designated by ΔB_ω in Table I.

2. Self-energy and vacuum polarization

The electron self energy and vacuum polarization were calculated using methods described in Ref. [63]. The only significant differences in the method described in that paper is that we include 17 partial waves here rather than 13 and carry out a more accurate evaluation of the vertex diagram in momentum space. To check the calculation, we let $U(r) = 0$, replaced $V_{\rm nuc}(r)$ with a Coulomb potential, and obtained good agreement with the values tabulated by Mohr and Kim for the $3s_{1/2}$ states [64] and by Mohr [65] for the $2p_{1/2}$ and $2p_{3/2}$ states. Explicit calculations were carried out at $Z = 25, 35, 50, 60, 70, 80$, and 90. Interpolation was used for intermediate Z values. Below $Z = 25$ scaled values of the Coulomb results were used. Because two-photon QED effects were not included, this part of the calculation has the largest theoretical error, which can be taken to be of order $1/Z$ of the Lamb shift. In Table I, we list the sum of the self-energy and vacuum polarization under the heading "QED."

D. Reduced mass and mass polarization

Reduced mass corrections are given by

$$\delta E_{RM} = -\frac{1}{M}\Big(E^{(0)} + E^{(1)} + E^{(2)} + E^{(3+)} + B^{(1)} + B^{(2)} + B^{(3+)} + \Delta B_{\omega}\Big) , \qquad (2.46)$$

where M is the nuclear mass in atomic units. Since this correction is included explicitly, the infinite mass Rydberg constant must be used to convert experimental energies to atomic units for comparison with our calculations. Additionally, we include mass-polarization corrections, which are also inversely proportional to the nuclear mass. Assuming that the nuclear motion is nonrelativistic, the mass-polarization corrections are obtained from the Hamiltonian

$$H_{\rm MP} = \frac{1}{M}\sum_{ijkl} p_{ijkl}\, a_i^{\dagger} a_j^{\dagger} a_l a_k, \qquad (2.47)$$

where

$$p_{ijkl} = \langle ij|\mathbf{p}_1 \cdot \mathbf{p}_2|kl\rangle .$$

This correction is calculated to first-order only. The sum of the first-order mass-polarization correction and the reduced-mass correction is designated by "RM" in Table I.

III. RESULTS

As a first step in our calculation, we solve the $V^{(N-1)}$ HF equations to obtain the $1s_{1/2}$, $2s_{1/2}$, $2p_{1/2}$, and $2p_{3/2}$ core orbitals and the $3s_{1/2}$, $3d_{3/2}$, and $3d_{5/2}$ valence orbitals. We then construct the unperturbed state vectors for $J = 0, 1$, and 2 states as linear combinations of particle-hole states having $a = 2p_{1/2}$ or $2p_{3/2}$ and $v = 3s_{1/2}$, $3d_{3/2}$, or $3d_{5/2}$. Next, the eigenvalue problem Eq. (2.30) is solved to give the lowest-order approximation for the expansion coefficients together with the energies $E^{(0)} + E^{(1)}$. In Fig. 1, we show the results of this preliminary calculation for $Z = 10 - 90$. From the upper panel of this figure, it is apparent that the $[2p_{3/2}^{-1}3s_{1/2}]_2$ state remains isolated from the four remaining states for all Z. By contrast, for $J = 1$, the two states $[2p_{1/2}^{-1}3s_{1/2}]_1$ and $[2p_{3/2}^{-1}3s_{1/2}]_1$ are nearly degenerate at low Z, while the states $[2p_{1/2}^{-1}3s_{1/2}]_1$, $[2p_{3/2}^{-1}3d_{3/2}]_1$, and $[2p_{3/2}^{-1}3d_{5/2}]_1$ interact strongly near $Z = 50$. From the lower panel, we see that the $[2p_{1/2}^{-1}3s_{1/2}]_0$ state is well isolated from the $[2p_{3/2}^{-1}3d_{3/2}]_0$ state except near $Z = 50$. With these observations in mind, we adopt the following computational scheme: For $J = 2$, we carry out a one-channel calculation starting from the configuration $[2p_{3/2}^{-1}3s_{1/2}]_2$. For $J = 1$, we carry out a two-channel calculation starting from configurations $[2p_{1/2}^{-1}3s_{1/2}]_1$ and $[2p_{3/2}^{-1}3s_{1/2}]_1$ except in the range $40 \leq Z \leq 60$, where we carry out a full five-channel calculation. For $J = 0$, we carry out a one-channel calculation starting from $[2p_{1/2}^{-1}3s_{1/2}]_0$ except in the range $40 \leq Z \leq 60$, where we carry out a two-channel calculation using configurations $[2p_{3/2}^{-1}3s_{1/2}]_0$ and $[2p_{3/2}^{-1}3d_{3/2}]_0$. In our discussion,

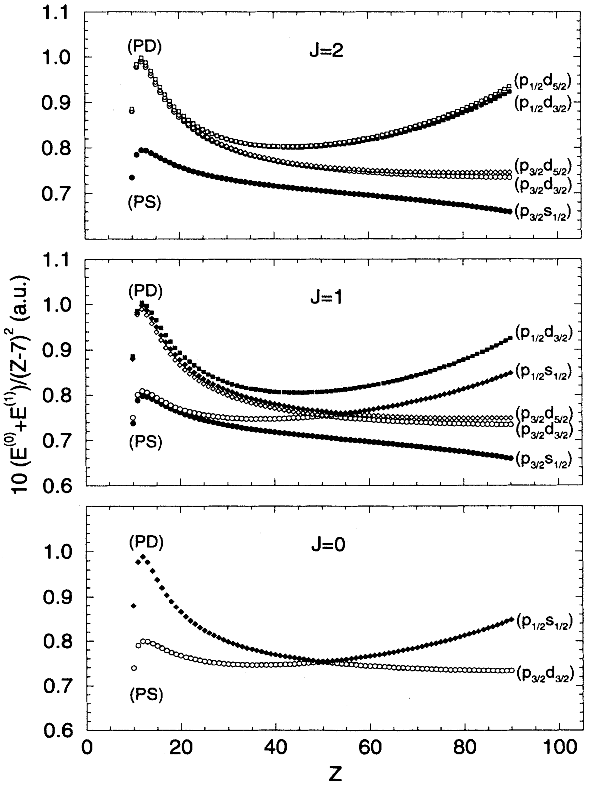

FIG. 1. Sum of the lowest- and first-order energies $E^{(0)} + E^{(1)}$ for the $J = 0$, $J = 1$, and $J = 2$ states of neonlike ions from a $V^{(N-1)}$ HF calculation. All states obtained by coupling a $2p$ hole with a $3s$ or $3d$ excited electron are shown.

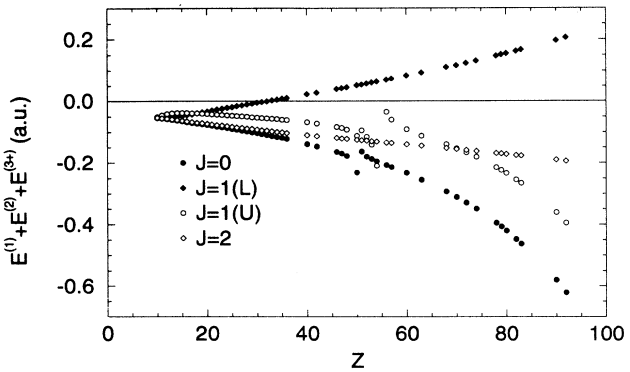

FIG. 2. Electrostatic correlation energy $E^{(1)}+E^{(2)}+E^{(3+)}$ for the $J=0$, $J=1$, and $J=2$ states of neonlike ions obtained from the iteration solution to the all-orders equations.

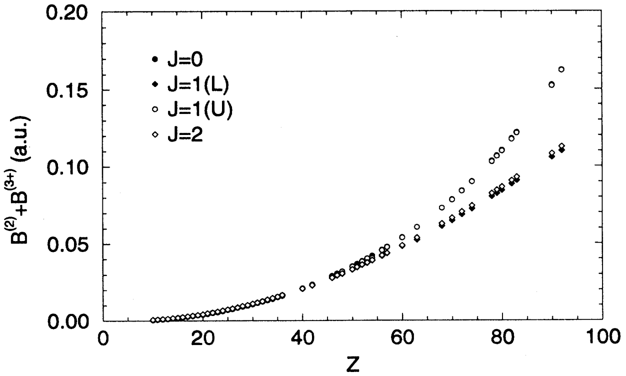

FIG. 4. Breit-Coulomb correlation corrections $B^{(2)}+B^{(3+)}$ for $[2p^{-1}3s]$ particle-hole states of neonlike ions.

we refer to the $[2p_{3/2}^{-1}3s_{1/2}]_1$ state as the $J=1(L)$ state and to the $[2p_{1/2}^{-1}3s_{1/2}]_1$ state as the $J=1(U)$ state. The labels (L) and (U) refer to lower and upper energy states. The values of $E^{(0)}+E^{(1)}$ obtained from such calculations are listed at intervals of $Z=10$ in Table I. The higher-order correlation corrections $E^{(2)}$ and $E^{(3+)}$ obtained by iterating the all-order equations are also listed in Table I and the total electrostatic correlation energy $E^{(1)}+E^{(2)}+E^{(3+)}$ is plotted against Z for each of the four states in Fig. 2. The irregularities in the correlation corrections for the two states $J=0$ and $J=1(U)$ seen in this figure are due to the near degeneracy of levels discussed above.

For highly charged ions, the largest correction to the energy is from the first-order Breit interaction $B^{(1)}$. This correction is shown in Fig. 3. Since the first-order Breit interaction is dominated by $(B_{\mathrm{HF}})_{aa}$, as discussed previously, the values are essentially independent of J and, as seen in the figure, the interaction energy depends principally on the hole state a. Numerical values of $B^{(1)}$ and the higher-order Breit-Coulomb corrections, $B^{(2)}$ and $B^{(3+)}$, are give in Table I and the sum $B^{(2)}+B^{(3+)}$ is plotted as a function of Z in Fig. 4. The frequency-dependent Breit correction ΔB_ω and the QED corrections are shown in Figs. 5 and 6, respectively. These corrections are also listed in Table I. Finally, the sum of the reduced-mass and mass-polarization corrections are given in Table I, along with the resulting theoretical energy levels.

In Table II, we give theoretical energies for each of the four $[2p^{-1}3s]_J$ states for the 46 ions considered here.

The previous calculation that is closest in approach to the present one is the nonrelativistic coupled-cluster calculation for neutral neon of Kaldor and Haque [49]. In that calculation, electrostatic correlation corrections were treated more completely than here, but relativistic and QED corrections were ignored. The predicted values of the two $J=1$ state energies were larger than those from the present calculation by about 0.001 a.u.; the energy of the singlet state agrees to four figures with experiment, while the triplet state energy disagrees with experiment at the 0.001 a.u. level. In the present calculation, the situation is reversed; the three triplet state energies agree with experiment at the 0.0002 a.u. level while the singlet state energy disagrees with experiment at the 0.001 a.u. level (Fig. 7).

We also find excellent agreement with the semiempirical calculations of Hibert, Le Dourneuf, and Mo-

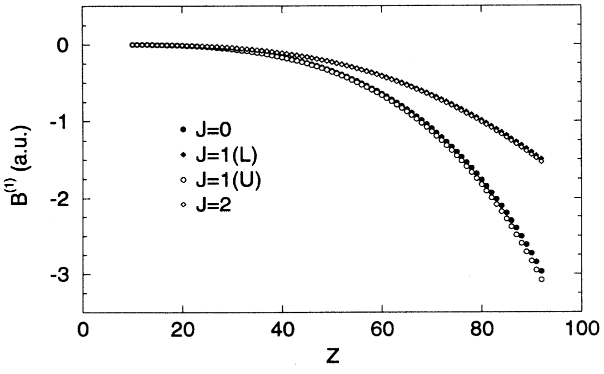

FIG. 3. Lowest-order Breit interaction $B^{(1)}$ for $[2p^{-1}3s]$ particle-hole states of neonlike ions.

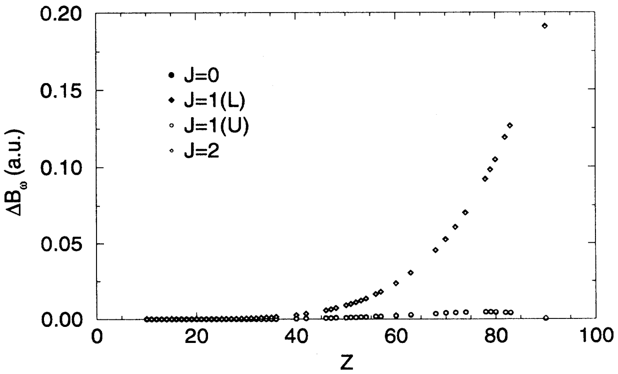

FIG. 5. Correction for frequency dependence of the Breit interaction ΔB_ω for $[2p^{-1}3s]$ particle-hole states of neonlike ions.

han [47] for their entire range of values $10 \leq Z \leq 36$; the disagreement being of order 0.005 a.u. throughout this range. Our calculations differ from the $1/Z$-expansion values of Safronova, Safronova, and Bruch [46] by amounts ranging from 0.001 a.u. at $Z = 18$ to 0.1 a.u. at $Z = 54$. We differ from the Dirac-Slater calculation of Sampson *et al.* [45] by amounts ranging between 0.03 a.u. for $Z = 26$ and 0.15 a.u. for $Z = 56$. Relatively good agreement is found with the MCDF calculations of Cogordan and Lunell [44] over their range $20 \leq Z \leq 54$; within this range, the differences increase from 0.01 to 0.04 a.u.. Differences from 0.03 to 0.05 a.u. are found with the relativistic configuration-interaction (CI) calculations of Kagawa, Honda, and Kiyokawa [50] over the range $18 \leq Z \leq 42$. Finally, we differ with the CI calculations of Biémont and Hansen [42] by 0.01–0.03 a.u.

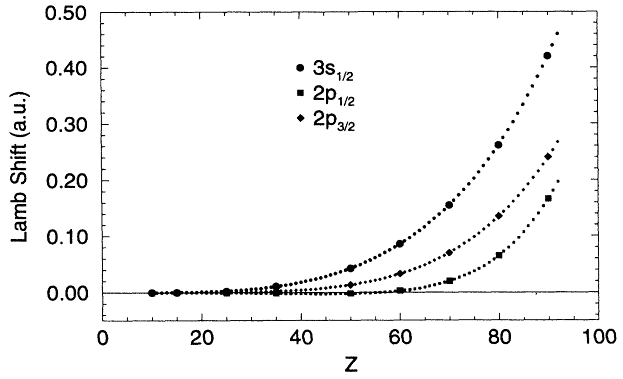

FIG. 6. QED corrections for $3s_{1/2}$, $2p_{1/2}$, and $2p_{3/2}$ states of neonlike ions.

TABLE II. Theoretical transition energies for the $[2p_{3/2}^{-1}3s_{1/2}]_2$, (2); $[2p_{3/2}^{-1}3s_{1/2}]_1$, (1L); $[2p_{1/2}^{-1}3s_{1/2}]_0$, (0); and $[2p_{1/2}^{-1}3s_{1/2}]_1$, (1U) states of neonlike ions. Units: a.u.

	Z	E	Z	E	Z	E	Z	E	Z	E	Z	E
(2)	10	0.6106	19	10.9295	28	32.3641	40	77.9112	54	154.7120	74	304.9550
	11	1.2062	20	12.7650	29	35.4247	42	87.3503	56	167.6783	78	340.0147
	12	1.9380	21	14.7375	30	38.6200	46	107.7796	57	174.3421	79	349.0045
	13	2.8079	22	16.8470	31	41.9497	47	113.2067	60	195.0447	80	358.0802
	14	3.8163	23	19.0931	32	45.4137	48	118.7611	63	216.7936	82	376.4766
	15	4.9630	24	21.4755	33	49.0114	50	130.2473	68	255.2821	83	385.7929
	16	6.2479	25	23.9941	34	52.7426	51	136.1780	70	271.4317	90	452.9223
	17	7.6708	26	26.6486	35	56.6069	52	142.2329	72	287.9936	92	472.6117
	18	9.2314	27	29.4387	36	60.6039	53	148.4111				
(1L)	10	0.6124	19	10.9642	28	32.4423	40	78.0450	54	154.9124	74	305.2643
	11	1.2096	20	12.8048	29	35.5075	42	87.4933	56	167.8886	78	340.3487
	12	1.9435	21	14.7823	30	38.7073	46	107.9413	57	174.5575	79	349.3449
	13	2.8161	22	16.8967	31	42.0417	47	113.3733	60	195.2755	80	358.4271
	14	3.8279	23	19.1477	32	45.5101	48	118.9323	63	217.0400	82	376.8366
	15	4.9786	24	21.5349	33	49.1124	50	130.4281	68	255.5561	83	386.1597
	16	6.2679	25	24.0583	34	52.8481	51	136.3637	70	271.7172	90	453.3390
	17	7.6955	26	26.7175	35	56.7170	52	142.4234	72	288.2908	92	473.0437
	18	9.2611	27	29.5122	36	60.7186	53	148.6065				
(0)	10	0.6140	19	11.0355	28	33.0161	40	81.1479	54	166.9939	74	355.9000
	11	1.2123	20	12.9007	29	36.1896	42	91.3705	56	182.1192	78	405.0692
	12	1.9479	21	14.9089	30	39.5120	46	113.7987	57	189.9696	79	418.0557
	13	2.8233	22	17.0604	31	42.9844	47	119.8278	60	214.7029	80	431.3328
	14	3.8392	23	19.3560	32	46.6075	48	126.0290	63	241.2701	82	458.7846
	15	4.9958	24	21.7961	33	50.3825	50	138.9368	68	289.8650	83	472.9748
	16	6.2933	25	24.3816	34	54.3102	51	145.7238	70	310.9010	90	581.7544
	17	7.7322	26	27.1129	35	58.3919	52	152.6224	72	332.8999	92	616.1665
	18	9.3128	27	29.9908	36	62.6285	53	159.7145				
(1U)	10	0.6177	19	11.0697	28	33.0620	40	81.2131	54	166.9801	74	356.0229
	11	1.2233	20	12.9361	29	36.2370	42	91.4384	56	182.2894	78	405.1932
	12	1.9647	21	14.9454	30	39.5609	46	113.8711	57	190.1113	79	418.1797
	13	2.8448	22	17.0982	31	43.0347	47	119.9012	60	214.8249	80	431.4568
	14	3.8642	23	19.3950	32	46.6593	48	126.1035	63	241.3873	82	458.9083
	15	5.0235	24	21.8365	33	50.4357	50	139.0258	68	289.9847	83	473.0982
	16	6.3232	25	24.4232	34	54.3649	51	145.7815	70	311.0219	90	581.8719
	17	7.7637	26	27.1560	35	58.4480	52	152.6736	72	333.0219	92	616.2809
	18	9.3458	27	30.0353	36	62.6860	53	159.7507				

TABLE III. Comparison of the present MBPT calculations of $[2p_{3/2}^{-1} 3s_{1/2}]_2$ energies (a.u.) for Ag^{37+}, Xe^{44+}, La^{47+}, Nd^{50+}, and Eu^{53+} with the MCDF calculations and experiments of Ref. [37].

	$E_{\rm Coulomb}$	$E_{\rm Breit}$	$E_{\rm QED}$	$E_{\rm Tot}$	$E_{\rm Expt}$	Δ(Theor−Expt)
Z=47 Ag^{37+}						
MBPT	113.337	−0.154	0.024	113.207		−0.008(6)
MCDF	113.305	−0.161	0.025	113.169	113.215(6)	−0.046(6)
Diff.	0.032	0.007	−0.001	0.038		
Z=54 Xe^{44+}						
MBPT	154.919	−0.244	0.038	154.712		−0.008(5)
MCDF	154.886	−0.253	0.040	154.673	154.720(5)	−0.047(5)
Diff.	0.033	0.009	−0.002	0.039		
Z=57 La^{47+}						
MBPT	174.588	−0.291	0.045	174.342		−0.010(7)
MCDF	174.556	−0.300	0.049	174.304	174.352(7)	−0.048(7)
Diff.	0.032	0.009	−0.004	0.038		
Z=60 Nd^{50+}						
MBPT	195.335	−0.343	0.053	195.045		−0.012(8)
MCDF	195.302	−0.352	0.057	195.006	195.057(8)	−0.051(8)
Diff.	0.033	0.009	−0.004	0.039		
Z=63 Eu^{53+}						
MBPT	217.132	−0.399	0.061	216.794		−0.019(21)
MCDF	217.099	−0.410	0.067	216.755	216.813(21)	−0.058(21)
Diff.	0.033	0.011	−0.006	0.039		

over their range of values $20 \leq Z \leq 34$.

For high Z, the most reliable calculations appear to be the 36 configuration MCDF calculations reported in Ref. [37]. In Table III, we compare values of the electrostatic, Breit, and QED contributions to the energies of the $J = 2$ states given in Ref. [37] with corresponding values from the present calculation. We find that the electrostatic energies of the four ions considered differ by 0.033 a.u., the Breit corrections differ by about 0.01 a.u., and the QED corrections differ by less than 0.006 a.u.. By including correlation corrections, the differences with experiment of 0.05 a.u. found in Ref. [37] are reduced to 0.01 a.u..

In Tables IV-VII, we compare in detail the theoretical and experimental energies. We see that the theoretical energies are systematically smaller than the experimental ones; the differences ranging from 0.001 a.u. near the neutral end to 0.01 a.u. near $Z = 54$, and then increasing more rapidly to ≈ 0.1 a.u. at $Z = 90$. In Fig. 8, we plot the differences between theory and experiment, together with the estimated error bars. These differences can be fitted by the weighted least squares polynomial, $-0.001636\zeta^2 + 0.000498\zeta^3 - 0.000047\zeta^4$ with $\zeta = Z/10$, which is also shown in the figure. The present calcu-

TABLE IV. Comparison of theoretical and experimental energies for the $[2p_{3/2}^{-1} 3s_{1/2}]_2$ state of neonlike ions. Units: (a.u.)

Z	Theory	Expt	Theor−Expt	Ref.
10	0.6106	0.6107	−0.0001	[1]
11	1.2062	1.2071	−0.0009	[19]
12	1.9380	1.9394	−0.0014	[1]
13	2.8079	2.8096(1)	−0.0017	[20]
14	3.8163	3.8183(1)	−0.0020	[4]
15	4.9630	4.9657(5)	−0.0027	[5]
16	6.2479	6.2503(5)	−0.0024	[6]
24	21.4755	21.479(9)	−0.003	[26]
26	26.6486	26.652(7)	−0.003	[11]
28	32.3641	32.368(20)	−0.004	[29,13]
29	35.4247	35.436(13)	−0.011	[14]
36	60.6039	60.602(9)	0.002	[16]
47	113.2067	113.215(6)	−0.008	[36]
54	154.7120	154.720(5)	−0.008	[37]
56	167.6783	167.688(7)	−0.010	[41]
57	174.3421	174.352(7)	−0.010	[37]
60	195.0447	195.057(8)	−0.012	[37]
63	216.7936	216.813(21)	−0.019	[37]
68	255.2821	255.317(7)	−0.035	[41]
72	287.9936	288.013(11)	−0.019	[41]
74	304.9550	304.998(14)	−0.043	[41]
78	340.0147	340.073(15)	−0.058	[41]
79	349.0045	349.070(32)	−0.065	[38,41]
80	358.0802	358.124(23)	−0.044	[41]
82	376.4766	376.504(19)	−0.027	[41]
90	452.9223	453.029(32)	−0.107	[40]

TABLE V. Comparison of theoretical and experimental energies for the $[2p_{3/2}^{-1}3s_{1/2}]_1$ state of neonlike ions. Units: a.u.

Z	Theory	Expt	Theor−Expt	Ref.	Z	Theory	Expt	Theor−Expt	Ref.
10	0.6124	0.6127	−0.0003	[1]	32	45.5101	45.518(22)	−0.008	[32]
11	1.2096	1.2106	−0.0010	[19]	33	49.1124	49.158(25)	−0.046	[33]
12	1.9435	1.9450	−0.0015	[2]	34	52.8481	52.890(28)	−0.042	[34]
13	2.8161	2.8180(1)	−0.0019	[3]	35	56.7170	56.740(32)	−0.023	[35]
14	3.8279	3.8300(1)	−0.0021	[4]	36	60.7186	60.720(9)	−0.001	[16]
15	4.9786	4.9814(5)	−0.0028	[5]	42	87.4933	87.573(140)	−0.080	[17,18]
16	6.2679	6.2705(5)	−0.0026	[6,7]	47	113.3733	113.381(6)	−0.008	[36]
17	7.6955	7.6977(20)	−0.0022	[21]	54	154.9124	154.919(5)	−0.007	[37]
18	9.2611	9.2646(5)	−0.0035	[22]	56	167.8886	167.895(7)	−0.006	[41]
19	10.9642	10.9683(18)	−0.0041	[23]	57	174.5575	174.572(13)	−0.015	[37]
20	12.8048	12.8074(30)	−0.0026	[24]	60	195.2755	195.291(8)	−0.015	[37]
21	14.7823	14.786(2)	−0.004	[8]	63	217.0400	217.072(21)	−0.032	[37]
22	16.8967	16.900(2)	−0.003	[25]	68	255.5561	255.585(14)	−0.029	[41]
23	19.1477	19.149(7)	−0.001	[9]	72	288.2908	288.308(11)	−0.017	[41]
24	21.5349	21.540(9)	−0.005	[26,10]	74	305.2643	305.303(14)	−0.039	[41]
25	24.0583	24.063(9)	−0.005	[27]	78	340.3487	340.398(18)	−0.049	[41]
26	26.7175	26.722(7)	−0.005	[11]	79	349.3449	349.412(32)	−0.067	[38,41]
27	29.5122	29.516(9)	−0.004	[12]	80	358.4271	358.448(23)	−0.021	[41]
28	32.4423	32.446(20)	−0.004	[29]	82	376.8366	376.837(19)	−0.000	[41]
29	35.5075	35.520(13)	−0.012	[14,15]	83	386.1597	386.155(44)	0.005	[39]
30	38.7073	38.715(10)	−0.008	[30]	90	453.3390	453.434(27)	−0.095	[40]
31	42.0417	42.060(20)	−0.018	[31]					

TABLE VI. Comparison of theoretical and experimental energies for the $[2p_{1/2}^{-1}3s_{1/2}]_0$ state of neonlike ions. Units: a.u.

Z	Theory	Expt	Theor−Expt	Ref.	Z	Theory	Expt	Theor−Expt	Ref.
10	0.6140	0.6143	−0.0003	[1]	15	4.9958	4.9986(5)	−0.0028	[5]
11	1.2123	1.2133	−0.0010	[19]	16	6.2933	6.2960(5)	−0.0027	[6]
12	1.9479	1.9495	−0.0016	[1]	26	27.1129	27.113(7)	−0.000	[28]
13	2.8233	2.8252(1)	−0.0019	[20]	29	36.1896	36.195(13)	−0.005	[14]
14	3.8392	3.8413(1)	−0.0021	[4]	36	62.6285	62.628(9)	0.000	[16]

TABLE VII. Comparison of theoretical and experimental energies for the $[2p_{1/2}^{-1}3s_{1/2}]_1$ state of neonlike ions. Units: a.u.

Z	Theory	Expt	Theor−Expt	Ref.	Z	Theory	Expt	Theor−Expt	Ref.
10	0.6177	0.6192	−0.0015	[1]	27	30.0353	30.037(9)	−0.002	[12]
11	1.2233	1.2246	−0.0013	[19]	28	33.0620	33.067(20)	−0.005	[29]
12	1.9647	1.9662	−0.0015	[2]	29	36.2370	36.246(13)	−0.009	[14,15]
13	2.8448	2.8464(1)	−0.0016	[3]	30	39.5609	39.565(10)	−0.004	[30]
14	3.8642	3.8661(1)	−0.0019	[4]	31	43.0347	43.053(22)	−0.018	[31]
15	5.0235	5.0262(5)	−0.0027	[5]	32	46.6593	46.675(23)	−0.016	[32]
16	6.3232	6.3257(5)	−0.0025	[6,7]	33	50.4357	50.434(27)	0.002	[33]
17	7.7637	7.7656(20)	−0.0019	[21]	34	54.3649	54.412(30)	−0.047	[34]
18	9.3458	9.3501(5)	−0.0043	[22]	35	58.4480	58.490(33)	−0.042	[35]
19	11.0697	11.0730(18)	−0.0033	[23]	36	62.6860	62.686(9)	0.000	[16]
20	12.9361	12.9395(30)	−0.0034	[24]	42	91.4384	91.491(140)	−0.053	[17,18]
21	14.9454	14.948(2)	−0.003	[8]	47	119.9012	119.894(6)	0.007	[36]
22	17.0982	17.103(2)	−0.005	[25]	54	166.9801	166.972(6)	0.008	[37]
23	19.3950	19.397(7)	−0.002	[9]	57	190.1113	190.125(8)	−0.014	[37]
24	21.8365	21.839(9)	−0.003	[26,10]	60	214.8249	214.861(15)	−0.036	[37]
25	24.4232	24.426(9)	−0.003	[27]	83	473.0982	473.114(55)	−0.016	[39]
26	27.1560	27.160(7)	−0.004	[11]					

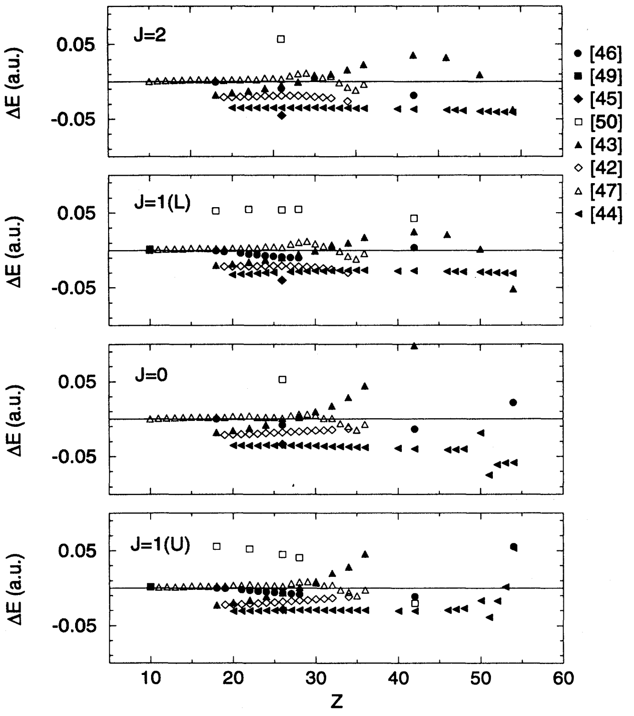

FIG. 7. Comparison of energies of the $J = 0, 1$, and 2 states of neonlike ions with other theories.

lation improves the agreement between *ab initio* theory and experiment for the isoelectronic sequence by roughly an order of magnitude.

We have no explanation for the residual differences between theory and experiment at high Z. They are most likely the result of our approximate treatment of the QED corrections. It should be noted that in another recent MBPT calculation of $2s \to 2p$ transitions in neonlike uranium, differences between theory and experiment of the same order of magnitude were found [57].

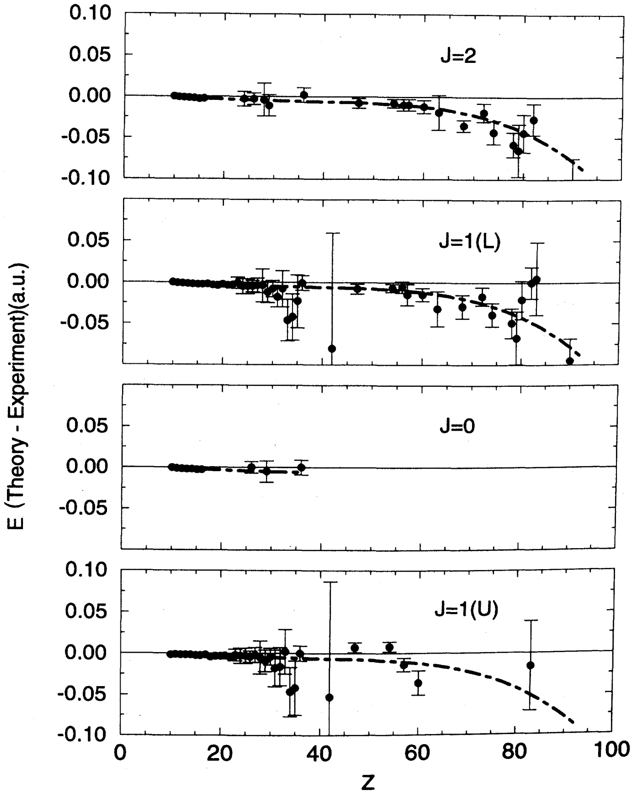

FIG. 8. Differences between theoretical and experimental energies for the $J = 0, 1$, and 2 states of neonlike ions. The dot-dashed curve represents a least-squares fit to the energy differences.

ACKNOWLEDGENTS

We would like to thank P. Beiersdorfer for permission to quote results of unpublished measurements. We also owe a debt of gratitude to W. Martin for a helpful discussion on errors in experimental measurements at low and intermediate Z. This research was supported in part by NSF Grant No. PHY-92-04089.

[1] C.E. Moore, *Atomic Energy Levels*, Natl. Bur. Stand. Ref. Data Ser., NBS (U.S.) Circ. No. 35 (U.S. GPO, Washington, D.C., 1971).

[2] V. Kaufman and W.C. Martin, J. Phys. Chem. Ref. Data **20**, 83 (1991).

[3] V. Kaufman and W.C. Martin, J. Phys. Chem. Ref. Data **20**, 775 (1991).

[4] W.C. Martin and R. Zalubas, J. Phys. Chem. Ref. Data **12**, 355 (1983).

[5] W.C. Martin, R. Zalubas, and A. Musgrove, J. Phys. Chem. Ref. Data **14**, 751 (1985).

[6] W.C. Martin, R. Zalubas, and A. Musgrove, J. Phys. Chem. Ref. Data **19**, 821 (1990).

[7] V. Kaufman and W.C. Martin, J. Phys. Chem. Ref. Data **22**, 279 (1993).

[8] V. Kaufman and J. Sugar, J. Phys. Chem. Ref. Data **17**, 1679 (1988).

[9] T. Shirai, T. Nakagaki, J. Sugar, and W.L. Wiese, J. Phys. Chem. Ref. Data **21**, 273 (1992).

[10] J. Sugar and Ch. Corliss, J. Phys. Chem. Ref. Data **6**, 317, 1253 (1977).

[11] T. Shirai, Y. Funatake, K. Mori, J. Sugar, W.L. Wiese, and Y. Nakai, J. Phys. Chem. Ref. Data **19**, 127 (1990).

[12] T. Shirai, A. Mengoni, Y. Nakai, J. Sugar, W.L. Wiese, K. Mori, and H. Sakai, J. Phys. Chem. Ref. Data **21**, 23 (1992).

[13] Ch. Corliss and J. Sugar, J. Phys. Chem. Ref. Data **10**, 197 (1981).

[14] J. Sugar and A. Musgrove, J. Phys. Chem. Ref. Data **19**, 527 (1990).

[15] T. Shirai, T. Nakagaki, Y. Nakai, J. Sugar, K. Ishii, and K. Mori, J. Phys. Chem. Ref. Data **20**, 1 (1991).

[16] J. Sugar and A. Musgrove, J. Phys. Chem. Ref. Data **20**, 859 (1991).

[17] T. Shirai, Y. Nakai, K. Ozawa, K. Ishii, J. Sugar, and K. Mori, J. Phys. Chem. Ref. Data **16**, 327 (1987).

[18] J. Sugar and A. Musgrove, J. Phys. Chem. Ref. Data **17**, 155 (1988).

[19] W.C. Martin and R. Zalubas, J. Phys. Chem. Ref. Data **10**, 164 (1981).

[20] W.C. Martin and R. Zalubas, J. Phys. Chem. Ref. Data **8**, 817 (1979).

[21] R.L. Kelly, J. Phys. Chem. Ref. Data **16**, Suppl. 1, 376 (1987).

[22] R.L. Kelly, J. Phys. Chem. Ref. Data **16**, Suppl. 1, 403 (1987).

[23] J. Sugar and C. Corliss, J. Phys. Chem. Ref. Data **14**, Suppl. 2, 36 (1985).

[24] J. Sugar and C. Corliss, J. Phys. Chem. Ref. Data **14**, Suppl. 2, 91 (1985).

[25] J. Sugar and C. Corliss, J. Phys. Chem. Ref. Data **14**, Suppl. 2, 186 (1985).

[26] J. Sugar and C. Corliss, J. Phys. Chem. Ref. Data **14**, Suppl. 2, 323 (1985).

[27] J. Sugar and C. Corliss, J. Phys. Chem. Ref. Data **14**, Suppl. 2, 395 (1985).

[28] J. Sugar and C. Corliss, J. Phys. Chem. Ref. Data **14**, Suppl. 2, 489 (1985).

[29] J. Sugar and C. Corliss, J. Phys. Chem. Ref. Data **14**, Suppl. 2, 651 (1985).

[30] R.L. Kelly, J. Phys. Chem. Ref. Data **16**, Suppl. 1, 1247 (1987).

[31] R.L. Kelly, J. Phys. Chem. Ref. Data **16**, Suppl. 1, 1262 (1987).

[32] J. Sugar and A. Musgrove, J. Phys. Chem. Ref. Data **22**, No. 5, 1269 (1993).

[33] R.L. Kelly, J. Phys. Chem. Ref. Data **16**, Suppl. 1, 1312 (1987).

[34] R.L. Kelly, J. Phys. Chem. Ref. Data **16**, Suppl. 1, 1332 (1987).

[35] R.L. Kelly, J. Phys. Chem. Ref. Data **16**, Suppl. 1, 1345 (1987).

[36] P. Beiersdorfer, M. Bitter, S. von Goeler, S. Cohen, K.W. Hill, J. Timberlake, R.S. Walling, M.H. Chen, P.L. Hagelstein, and J.H. Scofield, Phys. Rev. A **34**, 1297 (1986).

[37] P. Beiersdorfer, S. von Goeler, M. Bitter, E. Hinnov, R. Bell, S. Bernabei, J. Felt, K.W. Hill, R. Hulse, J. Stevens, S. Suckewer, J. Timberlake, A. Wouters, M.H. Chen, J.H. Scofield, D.D. Dietrich, M. Gerassimenko, E. Silver, R.S. Walling, and P.L. Hagelstein, Phys. Rev. A **37**, 4153 (1988).

[38] G.A. Chandler, M.H. Chen, D.D. Dietrich, P.O. Egan, K.P. Ziock, P.H. Mokler, S. Reusch, and D.H.H. Hoffmann, Phys. Rev. A **39**, 565 (1989).

[39] D.D. Dietrich, A. Simionovici, M.H. Chen, G. Chandler, C.J. Hailey, P.O. Egan, P.H. Mokler, S. Reusch, and D.H.H. Hoffmann, Phys. Rev. A **41**, 1450 (1990).

[40] P. Beiersdorfer, Nucl. Instrum. Methods B **56/57**, 1144 (1991).

[41] P. Beiersdorfer (private communication, 1994).

[42] E. Biémont and J.E. Hansen, At. Data Nucl. Data Tables **37**, 1 (1987).

[43] H. Zhang, D.H. Sampson, R.E.H. Clark, and J.B. Mann, At. Data Nucl. Data Tables **37**, 17 (1987).

[44] J.A. Cogordan and S. Lunell, Phys. Scr. **33**, 406 (1987).

[45] D.H. Sampson, H. Zhang, A.K. Mohanty, and R.E.H. Clark, Phys. Rev. A **40**, 604 (1989).

[46] U.I. Safronova, M.S. Safronova, and R. Bruch, Phys. Scr. **49**, 446 (1994).

[47] A. Hibert, M. Le Dourneuf, and M. Mohan, At. Data Nucl. Data Tables **53**, 23 (1993).

[48] A. Hibert and M.P. Scott, J. Phys. B **37**, 1315 (1994).

[49] U. Kaldor and A. Haque, Chem. Phys. Lett. **128**, 45 (1987).

[50] T. Kagawa, Y. Honda, and Sh. Kiyokawa, Phys. Rev. A **44**, 7092 (1991).

[51] E. Avgoustoglou, W.R. Johnson, D.R. Plante, J. Sapirstein, S. Sheinerman, and S.A. Blundell, Phys. Rev. A **46**, 5478 (1992).

[52] F. Paschen, Ann. Phys. **63**, 201 (1920).

[53] I. Lindgren and D. Mukherjee, Phys. Rep. **151**, 93 (1987).

[54] I. Lindgren and J. Morrison, *Atomic Many-Body Theory*, 2nd ed. (Springer-Verlag, Berlin, 1986).

[55] See review by D. Mukherjee and S. Pal, Adv. Quantum Chem. **20**, 291 (1987).

[56] H.P. Kelly, At. Phys. **8**, 305 (1983); Phys. Scr. **T17**, 109 (1987).

[57] W.R. Johnson, J. Sapirstein, and K.T. Cheng, Phys. Rev. A **51**, 297 (1995).

[58] J. Sucher, Phys. Rev. A **22**, 348 (1980).

[59] W.R. Johnson and G. Soff, At. Data Nucl. Data Tables **33**, 405 (1985).

[60] A. Fetter and J. Walecka, *Quantum Theory of Many-Particle Systems* (McGraw-Hill, New York, 1971).

[61] Z.W. Liu and H.P. Kelly, Phys. Rev. A **43**, 3305 (1991).

[62] W.R. Johnson, S.A. Blundell, and J. Sapirstein, Phys. Rev. A **37**, 307 (1988).

[63] K.T. Cheng, W.R. Johnson, and J. Sapirstein, Phys. Rev. A **47**, 1817 (1993).

[64] P.J. Mohr and Y.-K. Kim, Phys. Rev. A **45**, 2727 (1992).

[65] P.J. Mohr, Phys. Rev. A **46**, 4421 (1992).